How Cats Lap: Water Uptake by *Felis catus*

Pedro M. Reis, *et al.*

Science **330**, 1231 (2010);
DOI: 10.1126/science.1195421

location core, which occurs in the plane with relatively weak bonding (that is, between the upper and lower layers of the puckered Al layer). As no charge transport is involved, the Peierls barriers are smaller than if the dislocations were charged.

It is not clear whether the core structure of glissile basal dislocations shown in Fig. 3 should be expected for dislocations present in a low-angle boundary (*9*). The periodic electrostatic and stress fields present in such a boundary could well lead to a different core structure for its constituent dislocations.

The NCSI studies have also revealed a stacking fault on the basal plane (fig. S4), but only in the thinnest regions of the TEM foils; such faults have not been reported for α-Al_2O_3 as yet. Partial dislocations are present at the ends of the three distinct faults in this image. At the dislocation cores, similar contrast to that of the dislocation core in Fig. 2A is observed: Low contrast occurs in the puckered Al layer. The details of the contrast feature of the experimental image have been reproduced in the calculated image, indicating a rearrangement of the Al atoms in the puckered layer (fig. S5) (*7*).

The NCSI technique has been used to image, at atomic resolution, partial dislocations bounding prism-plane stacking faults in sapphire deformed at high temperatures. The dislocations appear to be stoichiometric and uncharged, and the cores exhibit 50% occupancy of the Al cations to achieve electrical neutrality. Because of core spreading, the Al ions at the termination of the extra half planes exhibit random occupancy of sites showing tetrahedral and octahedral coordination. It is likely that the motion plane is within the puckered Al sublattice, following the Bilde-Sørensen *et al*. model (*8*) for gliding basal dislocations.

References and Notes

1. J. B. Wachtman Jr., I. H. Maxwell, *J. Am. Ceram. Soc.* **37**, 291 (1954).
2. M. L. Kronberg, *Acta Metall.* **5**, 507 (1957).
3. A. G. Marinopoulos, C. Elsässer, *Philos. Mag. Lett.* **81**, 329 (2001).
4. M. H. Jhon, A. M. Glaeser, D. C. Chrzan, *Phys. Rev. B* **71**, 214101 (2005).
5. K. P. D. Lagerlöf, J. Castaing, A. H. Heuer, *Philos. Mag.* **89**, 489 (2009).
6. Actually, the conventional concept of a well-defined stacking fault with a well-defined SFE may break down when the energy is as high as it is for sapphire on the basal plane. The configuration in Fig. 1A (ii) should be thought of as an extended core.
7. Supporting material is available on *Science* Online.
8. J. B. Bilde-Sørensen *et al*., *Acta Mater.* **44**, 2145 (1996).
9. N. Shibata *et al*., *Science* **316**, 82 (2007).
10. C. L. Jia, M. Lentzen, K. Urban, *Science* **299**, 870 (2003).
11. K. P. D. Lagerlöf *et al*., *Acta Metall.* **32**, 97 (1984).
12. Theoretical density functional theory calculations (*4*) yielded (0 K) values of 0.42 or 0.35 J/m^2, depending on the computational scheme that was employed (local density approximation or generalized gradient approximation). This difference from the experimental value might be due to the neglect of temperature effects in the calculations. Shell-model calculations (*4*) of SFEs indicate reductions of 0.1 to 0.2 J/m^2 between 0 and 1800 K due to vibrational entropy effects.
13. The small difference between the SFE calculated from the separation of the dissociated edge and 30° partials is possibly due to the partials not having reached their equilibrium separation.
14. D. B. Williams, C. B. Carter, *Transmission Electron Microscopy* (Springer, Berlin, ed. 2, 2009).
15. C. L. Jia *et al*., *Nat. Mater.* **7**, 57 (2008).
16. J. D. Eshelby, A. N. Stroh, *Philos. Mag.* **42**, 1401 (1951).
17. As discussed in the SOM (fig. S3), the simulations of the dislocation core structure with and without consideration of the Eshelby twist (fig. S3, B and C) are indistinguishable. This arises because of the very small displacements involved in the Eshelby twist (which displacements are not included in Fig. 2, C and D, but were included in Fig. 2B to allow comparison with the experimental image).
18. Although $\alpha - Al_2O_3$ has a trigonal crystal structure (space group no. 167: $R\bar{3}c$, where R is the rhombohedral space lattice), it is remarkably isotropic elastically {the anisotropy factor is approximately $A = 0.857$ [see, for example, (*19*)]}. Hence, the Eshelby-Stroh formula, which applies to elastic isotropic solids, can be used to a first approximation.
19. D. S. Phillips, T. E. Mitchell, A. H. Heuer, *Philos. Mag. A* **45**, 1371 (1982).
20. Note that the dislocations are again portrayed to have dissociated to a width of ~2**b**, and the cores of both partials have undergone core spreading.

21. We are grateful to L. Houben (ER-C, Jülich, Germany) for his help in modeling the Eshelby twist for the 60° partial dislocation and to K. Urban (ER-C, Jülich, Germany), M. Rühle (Max Planck Institute for Metals Research, Stuttgart, Germany), F. Ernst [Case Western Reserve Univ. (CWRU), Cleveland, OH], and P. Pirouz (CWRU, Cleveland, OH) for useful discussions.

Supporting Online Material

www.sciencemag.org/cgi/content/full/330/6008/1227/DC1
SOM Text
Figs. S1 to S5
References

14 May 2010; accepted 27 October 2010
10.1126/science.1192319

How Cats Lap: Water Uptake by *Felis catus*

Pedro M. Reis,[1,2]* Sunghwan Jung,[3]* Jeffrey M. Aristoff,[4]* Roman Stocker[1]*†

Animals have developed a range of drinking strategies depending on physiological and environmental constraints. Vertebrates with incomplete cheeks use their tongue to drink; the most common example is the lapping of cats and dogs. We show that the domestic cat (*Felis catus*) laps by a subtle mechanism based on water adhesion to the dorsal side of the tongue. A combined experimental and theoretical analysis reveals that *Felis catus* exploits fluid inertia to defeat gravity and pull liquid into the mouth. This competition between inertia and gravity sets the lapping frequency and yields a prediction for the dependence of frequency on animal mass. Measurements of lapping frequency across the family Felidae support this prediction, which suggests that the lapping mechanism is conserved among felines.

Terrestrial animals have evolved diverse means to acquire water, including absorption through the skin (*1*) or extraction of moisture from food (*2*), but most rely on drinking (*3*–*12*). Drinking presents a challenge to land vertebrates, because fresh water occurs mainly as horizontal liquid surfaces, such as puddles, ponds, lakes, or streams, and animals must displace water upward against gravity to drink it. Crucial in the drinking process is the role of the tongue, which in vertebrates is used in two distinctly different ways. Vertebrates with complete cheeks, such as pigs, sheep, and horses, use suction to draw liquid upward and use their tongue to transport it intraorally (*13*, *14*). In contrast, vertebrates with incomplete cheeks, including most carnivores, are unable (after weaning) to seal their mouth cavity to generate suction and must rely on their tongue to move water into the mouth (*13*). When the tongue sweeps the bottom of a shallow puddle, the process is called licking (*4*). When the puddle is deeper than the tongue excursion into the liquid, it is called lapping (*15*). Here, we report on the lapping mechanism of the domestic cat (*Felis catus*).

Almost everyone has observed a domestic cat lap milk or water. Yet casual observation hardly captures the elegance and complexity of this act, as the tongue's motion is too fast to be resolved by the naked eye. We used high-speed imaging to capture the motion of both the tongue and liquid during lapping [Fig. 1 and movie S1 (*16*)]. With the cat's face oriented downward, the tongue extends from the jaw (Fig. 1A) and its tip curls sharply caudally (Fig. 1B). At the lowest position of the tongue's tip, its dorsal side rests on the liquid surface, without piercing it (Fig. 1B). When the cat lifts the tongue, liquid adhering to the dorsal side of the tip is drawn upward, forming a column (Fig. 1C). This liquid column is further extended by the tongue's upward motion (Fig. 1D), thinning in the process (Fig. 1E), and is finally partially captured upon jaw closure (Fig. 1, E and F). Inside the mouth, cavities

[1]Department of Civil and Environmental Engineering, Massachusetts Institute of Technology (MIT), Cambridge, MA 02139, USA. [2]Department of Mechanical Engineering, MIT, Cambridge, MA 02139, USA. [3]Department of Engineering Science and Mechanics, Virginia Polytechnic Institute and State University, Blacksburg, VA 24061, USA. [4]Department of Mechanical and Aerospace Engineering, Princeton University, Princeton, NJ 08544, USA.

*All authors contributed equally to this work.
†To whom correspondence should be addressed. E-mail: romans@mit.edu

between the palate's rugae and the tongue act as a nonreturn device and trap liquid until it is ingested every 3 to 17 cycles (*15*).

This sequence of events reveals two important aspects of how *F. catus* laps. First, lapping does not rely on "scooping" water into the mouth as in dogs (*Canis lupus familiaris*). Although the dog's tongue also curls caudally in a cuplike shape, it penetrates the liquid surface and scoops up the water that fills its ventral side. In contrast, the cat's tongue does not dip into the liquid (Fig. 1B) and the cavity on its ventral side remains empty (Fig. 1, B and C), as also recognized in a 1940 Oscar-winning short film (*17*). Second, only the tip of the tongue is used for lapping. The tip is free of filiform papillae (*18*) (Fig. 1G), the semirigid hairlike structures that give a cat's tongue its characteristic roughness. Thus, papillae appear to have no function in lapping.

The movies allowed us to quantify the lapping kinematics. The position of the tip of the tongue was tracked over one lapping event (Fig. 2A) and averaged over 11 cycles (Fig. 2B). The tongue's vertical position during upward motion is well described by an error-function profile, $Z(t) = \frac{1}{2}H\{1 + \mathrm{erf}(U_{MAX}t\sqrt{\pi}/H)\}$, where $H = 3.0$ cm (Fig. 2B, red) is the total vertical displacement, U_{MAX} is the maximum speed, and t is the time measured with respect to $Z(t{=}0) = H/2$, the half-height. As a result, the vertical velocity has an approximately Gaussian profile (Fig. 2B, blue): The tongue accelerates as it leaves the water surface, attains a remarkable maximum speed of $U_{MAX} = 78 \pm 2$ cm s^{-1}, then decelerates as it enters the mouth. Recordings of 10 adult individuals (*16*) yielded a lapping frequency $f = 3.5 \pm 0.4$ s^{-1} and an ingested volume per lap $V = 0.14 \pm 0.04$ ml.

To help understand the mechanism of lapping, we performed physical experiments in which a glass disk of radius R (representing the tongue's tip), initially placed on a water surface, was pulled vertically upward (Fig. 3). The time series of the disk position was set by a computer-controlled stage and programmed to have the observed error-function profile (Fig. 2B), where we could control the lapping height H and speed U_{MAX}. The hydrophilic nature of glass (static contact angle = 14°) mimicked the wetness of the tongue. High-speed imaging revealed the formation and extension of a water column, as in lapping (Fig. 3, A to G and movies S2 and S3) (*16*). The column's ascent was eventually interrupted by pinch-off, leaving a pendantlike drop on the lower surface of the disk (Fig. 3, F to H).

Estimation of the forces involved suggests that the fluid dynamics of lapping are governed by inertia and gravity, whereas viscous and capillary forces are negligible (*16*). Inertial entrainment draws liquid upward into a column, while gravity acts to collapse it. Ultimately, gravity prevails and the column pinches off. Dimensional analysis reveals that two dimensionless parameters control lapping: the Froude number, $\mathrm{Fr} = U_{MAX}/(gR)^{1/2}$, measuring the relative importance of inertia and gravity (g is the gravitational acceleration), and the aspect ratio, H/R. Experiments were therefore conducted over a range of Fr and H/R values (*16*), for a fixed lapping height, $H =$ 3 cm, determined from observations (Fig. 2B). The latter is possibly dictated by biological constraints, such as the need to keep whiskers dry to maintain their sensory performance (*19*) or to maximize peripheral vision while drinking.

To test the proposition that the column dynamics are set by a competition between inertia and gravity, we compared the height of the disk (Z) at pinch-off, Z_P, with that predicted from our scaling analysis. We find (*16*) that $Z_P/H \sim \mathrm{Fr}^*$ for $\mathrm{Fr}^* < 1$ and $Z_P/H \sim 1$ otherwise. Here, $\mathrm{Fr}^* = (R/H)\mathrm{Fr}^{2/3}$ is the ratio of the time scale for the gravitational collapse of the column, $t_P = (R/U_{MAX})\mathrm{Fr}^{2/3}$, and the time scale for the upward motion of the disk, H/U_{MAX}. Experiments confirmed the existence of two regimes (Fig. 4A). For small disks ($R = 2.5$ and 5 mm), Z_P/H increased linearly with Fr*, whereas large disks (R = 10 and 12.7 mm) reached the final height before pinch-off ($Z_P/H =$ 1). Theory also successfully predicts that pinch-off occurs close to the disk (Fig. 3).

Consequently, the balance between inertia and gravity dictates the lapping frequency, f, by controlling the time of pinch-off. To maximize ingested volume, which is assumed to be proportional to the column's volume V, the lapping time, $1/f$, should match the pinch-off time, t_P, because faster lapping fails to maximize inertial entrainment, whereas slower lapping results in belated mouth closure that misses most of the column. This predicts $f \sim (gH)^{1/2}/R$ or, because $f \sim U_{MAX}/H$, that Fr* is of order one. For domestic cats, we find that Fr* is indeed of order unity (0.4), using the experimentally measured values $U_{MAX} = 78$ cm s^{-1} and $H = 3$ cm (Fig. 2B) and a tongue size of $R \approx$ 5 mm (Fig. 1G).

The growth dynamics of the column's volume (Fig. 4B) (*16*) provide further evidence that the lapping frequency is set by the interplay between inertia and gravity. When the disk is close to the bath ($Z << H$), the column is cylindrical and V increases as $V/R^3 = \pi Z/R$ (Fig. 4B inset). Gravity-driven drainage then reduces the rate of volume increase, and V is at a maximum when gravity and inertia balance (Fig. 4B). A scaling argument predicts a maximum volume when the disk height reaches $Z_{MaxVol}/H \sim \mathrm{Fr}^*$ (*16*), in excellent agreement with observations (Fig. 4A). This also supports our assumption that V is maximum close to the time of pinch-off. In fact, V always peaks shortly before pinch-off (10 to 70 ms) (Fig. 4B), which suggests that mouth closure should also occur just before pinch-off to maximize captured volume. Observations of domestic cats showed that mouth closure indeed typically preceded pinch-off (movie S1) (*16*).

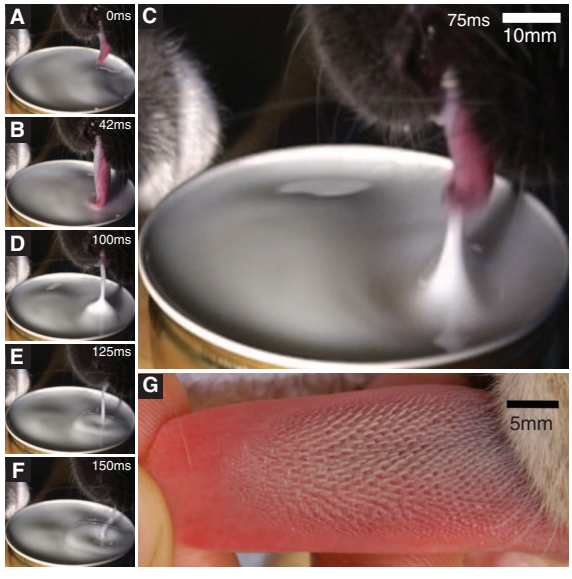

Fig. 1. The lapping process. (**A** to **F**) Snapshots showing the movement of the tongue of *F. catus* and the dynamics of the liquid column during a lapping cycle. Lapping occurs by fluid adhesion to the dorsal part of the tongue's tip and by lifting a liquid column through the tongue's upward motion, before jaw closure. Time elapsed from the first frame is given in the top left corner of each frame. (**G**) Photograph of the dorsal side of the tongue of *F. catus*, acquired under anesthesia (*16*). Only the smooth tip is used in lapping.

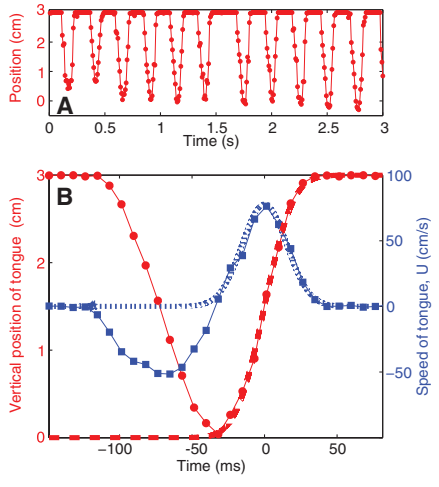

Fig. 2. The lapping kinematics. (**A**) Vertical position of the tip of the tongue of *F. catus* over 11 lapping cycles. (**B**) Vertical position (red circles) and velocity (blue squares) of the tongue's tip during a typical lapping cycle, obtained by averaging 11 cycles. The dashed line (red) represents a fitted error-function profile for vertical position. The dotted line (blue) is its temporal derivative and represents upward speed, which yielded $U_{MAX} = 78 \pm 2$ cm s^{-1}.

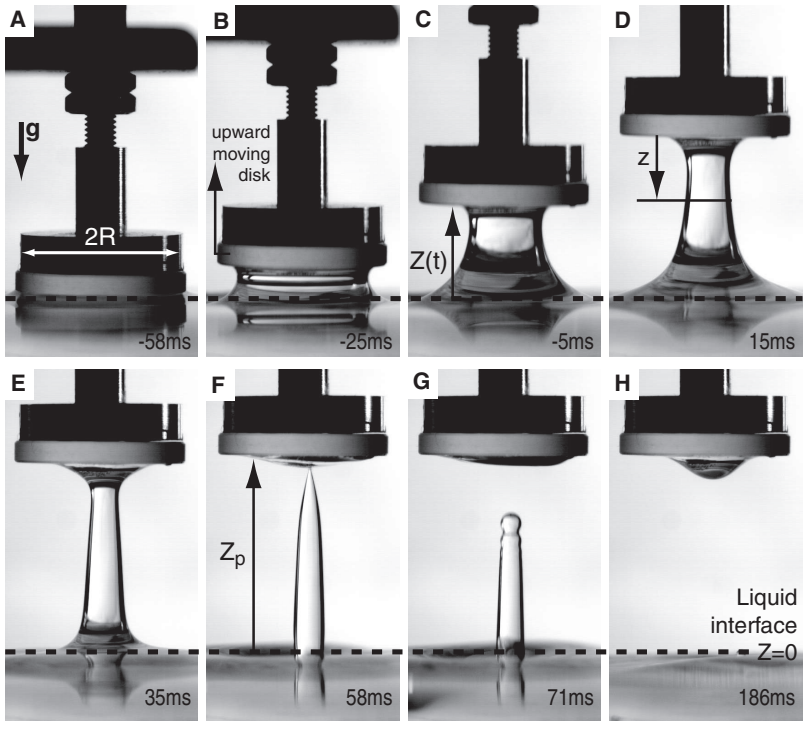

Fig. 3. Physical model of lapping. A disk of radius R is driven vertically upward, such that the elevation of the disk, $Z(t)$, from the liquid interface (dashed line, $Z = 0$), has an error-function profile (*16*). Lowercase z denotes the distance of a generic liquid layer from the disk. The sequence illustrates the formation (**A** to **E**) and pinch-off (**F**) of the liquid column. After pinch-off, part of the column collapses into the bath (**G**), which leaves a pendantlike drop attached to the disk (**H**). The final height of the disk is $Z = H$. Time is measured relative to the moment the disk reaches height $Z = H/2 = 1.5$ cm. This sequence corresponds to $R = 12.7$ mm, $H = 3$ cm, $U_{MAX} = 50$ cm s^{-1} (Fr = 1.42; Fr* = 0.60).

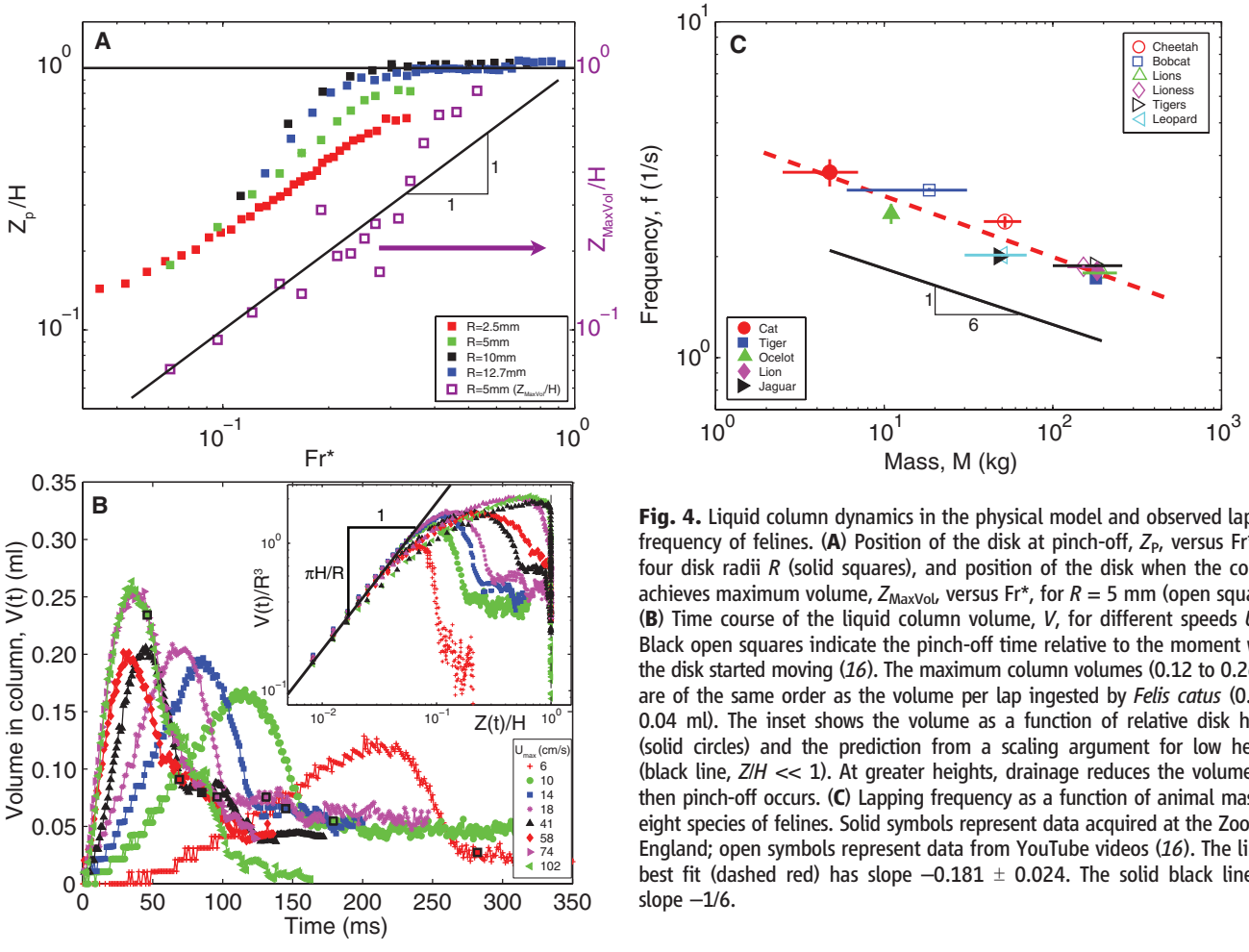

Fig. 4. Liquid column dynamics in the physical model and observed lapping frequency of felines. (**A**) Position of the disk at pinch-off, Z_P, versus Fr*, for four disk radii R (solid squares), and position of the disk when the column achieves maximum volume, Z_{MaxVol}, versus Fr*, for $R = 5$ mm (open squares). (**B**) Time course of the liquid column volume, V, for different speeds U_{MAX}. Black open squares indicate the pinch-off time relative to the moment when the disk started moving (*16*). The maximum column volumes (0.12 to 0.26 ml) are of the same order as the volume per lap ingested by *Felis catus* (0.14 ± 0.04 ml). The inset shows the volume as a function of relative disk height (solid circles) and the prediction from a scaling argument for low heights (black line, $Z/H << 1$). At greater heights, drainage reduces the volume and then pinch-off occurs. (**C**) Lapping frequency as a function of animal mass for eight species of felines. Solid symbols represent data acquired at the Zoo New England; open symbols represent data from YouTube videos (*16*). The line of best fit (dashed red) has slope −0.181 ± 0.024. The solid black line has slope −1/6.

The balance of inertia and gravity yields a prediction for the lapping frequency of other felines. Assuming isometry within the Felidae family (i.e., that lapping height H scales linearly with tongue width R and animal mass M scales as R^3), the finding that Fr* is of order one translates to the prediction $f \sim R^{-1/2} \sim M^{-1/6}$. Isometry or marginally positive allometry among the Felidae has been demonstrated for skull (*20*, *21*) and limb bones (*22*). Although variability by function can lead to departures from isometry in interspecific scalings (*23*), reported variations within the Felidae (*23*, *24*) only minimally affect the predicted scaling $f \sim M^{-1/6}$. We tested this –1/6 power-law dependence by measuring the lapping frequency for eight species of felines, from videos acquired at the Zoo New England or available on YouTube (*16*). The lapping frequency was observed to decrease with animal mass as $f = 4.6\ M^{-0.181 \pm 0.024}$ (f in s^{-1}, M in kg) (Fig. 4C), close to the predicted $M^{-1/6}$. This close agreement suggests that the domestic cat's inertia- and gravity-controlled lapping mechanism is conserved among felines.

The lapping of *F. catus* is part of a wider class of problems in biology involving gravity and inertia, sometimes referred to as Froude mechanisms. For example, the water-running ability of the Basilisk lizard depends on the gravity-driven collapse of the air cavity it creates upon slapping the water surface with its feet. The depth to which the lizard's leg penetrates the surface depends on the Froude number, which in turn prescribes the minimum slapping frequency (*25*). The Froude number is also relevant to swimming, for example, setting the maximum practical swimming speed in ducks (*26*), and to terrestrial legged locomotion. In this respect, it is interesting to note that the transition from trot to gallop obeys nearly the same scaling of frequency with mass as lapping, $f = 4.5\ M^{-0.14}$ (f in s^{-1}, M in kg) (*27*).

The subtle use of the tongue in the drinking process of *F. catus* is remarkable, given the tongue's lack of skeletal support (*28*). Complex movement in the absence of rigid components is a common feature of muscular hydrostats, which in addition to tongues include elephant trunks and octopus arms (*28*, *29*). The functional diversity and high compliance of these structures continue to inspire the design of soft robots (*29*), and a fundamental understanding of their functionality can lead to new design concepts and is essential to inform biomechanical models (*29*, *30*).

References and Notes

1. P. J. Bentley, T. Yorio, *J. Exp. Biol.* **79**, 41 (1979).
2. D. Attenborough, *The Living Planet: A Portrait of the Earth* (Collins and British Broadcasting Corporation, London, 1984).
3. J. Heidweiller, J. A. van Loon, G. A. Zweers, *Zoomorphology* **111**, 141 (1992).
4. J. A. W. M. Weijnen, *Neurosci. Biobehav. Rev.* **22**, 751 (1998).
5. W. C. Dilger, in *Roots of Behavior*, E. L. Bliss, Ed. (Harper, New York, 1962), pp. 35–47.
6. M. Prakash, D. Quéré, J. W. M. Bush, *Science* **320**, 931 (2008).
7. S. W. S. Gussekloo, R. G. Bout, *J. Exp. Biol.* **208**, 3395 (2005).
8. T. L. Daniel, J. G. Kingsolver, E. Meyhöfer, *Oecologia* **79**, 66 (1989).
9. J. G. Kingsolver, T. L. Daniel, *Oecologia* **60**, 214 (1983).
10. D. Cundall, *J. Exp. Biol.* **203**, 2171 (2000).
11. J. Heidweiller, G. A. Zweers, *Condor* **92**, 1 (1990).
12. J. G. M. Kooloos, G. A. Zweers, *J. Morphol.* **199**, 327 (1989).
13. A. J. Thexton, A. W. Crompton, R. Z. German, *J. Exp. Zool.* **280**, 327 (1998).
14. K. M. Hiiemae, A. W. Crompton, in *Functional Vertebrate Morphology*, M. Hildebrand, D. Bramble, K. Liem, D. B. Wake, Eds. (Belknap of Harvard Univ. Press, Cambridge, MA, 1985), pp. 262–290.
15. A. J. Thexton, J. D. McGarrick, *Arch. Oral Biol.* **33**, 331 (1988).
16. Materials and methods are available as supporting material on *Science* Online.
17. *Quicker 'n a Wink* (Metro-Goldwyn-Mayer Studios, Los Angeles, CA, 1940); www.youtube.com/watch?v=jUZwFrGzQGw.
18. K. Ojima, F. Mitsuhashi, M. Nasu, Y. Suzuki, *Ann. Anat.* **182**, 47 (2000).
19. A. S. Ahl, *Vet. Res. Commun.* **10**, 245 (1986).
20. P. Christiansen, J. S. Adolfssen, *J. Zool. (London)* **266**, 133 (2005).
21. A. P. Russell, H. N. Bryant, G. L. Powell, R. Laroiya, *J. Zool. (London)* **236**, 161 (1995).
22. J. Meachen-Samuels, B. Van Valkenburgh, *J. Morphol.* **270**, 729 (2009).
23. M. Doube, A. Wiktorowicz-Conroy, P. Christiansen, J. R. Hutchinson, S. Shefelbine, *PLoS ONE* **4**, e4742 (2009).
24. L. M. Day, B. C. Jayne, *J. Exp. Biol.* **210**, 642 (2007).
25. J. W. Glasheen, T. A. Mcmahon, *J. Exp. Biol.* **199**, 2611 (1996).
26. H. D. Prange, K. Schmidt-Nielsen, *J. Exp. Biol.* **53**, 763 (1970).
27. N. C. Heglund, C. R. Taylor, T. A. McMahon, *Science* **186**, 1112 (1974).
28. K. K. Smith, W. M. Kier, *Am. Sci.* **77**, 28 (1989).
29. D. Trivedi, C. D. Rahn, W. M. Kier, I. D. Walker, *Appl. Bionics Biomech.* **5**, 99 (2008).
30. H. J. Chiel, P. Crago, J. M. Mansour, K. Hathi, *Biol. Cybern.* **67**, 403 (1992).

31. All research with animals complied with and was approved by MIT's Animal Rights Committee. We thank J. Piazza and the staff at the Zoo New England for help with filming felines; M. Rock, A. Kennedy, and the Massachusetts Society for the Prevention of Cruelty to Animals (MSPCA) for help with filming domestic cats; G. McKinley for use of his FiSER stage; A. Crompton, A. Thexton, W. Kier, J. Bales, J. Bush, B. Andreotti, J. Bico, D. Vella, and A. Boudaoud for discussions and comments; and A. Jones, E. Samaha, R. Tomas, and W. Jarjoui for technical assistance. S.J., P.M.R., and R.S. designed research; S.J., P.M.R., R.S., and J.M.A. performed experiments and analyzed data; S.J., J.M.A., and R.S. developed scalings and theory; P.M.R., R.S., S.J., and J.M.A. wrote the paper.

Supporting Online Material

www.sciencemag.org/cgi/content/full/330/6008/1231/DC1
Materials and Methods
References
Movies S1 to S3

21 July 2010; accepted 20 October 2010
10.1126/science.1195421

Reducing the Gender Achievement Gap in College Science: A Classroom Study of Values Affirmation

Akira Miyake,[1]* Lauren E. Kost-Smith,[2] Noah D. Finkelstein,[2] Steven J. Pollock,[2] Geoffrey L. Cohen,[3] Tiffany A. Ito[1]

In many science, technology, engineering, and mathematics disciplines, women are outperformed by men in test scores, jeopardizing their success in science-oriented courses and careers. The current study tested the effectiveness of a psychological intervention, called values affirmation, in reducing the gender achievement gap in a college-level introductory physics class. In this randomized double-blind study, 399 students either wrote about their most important values or not, twice at the beginning of the 15-week course. Values affirmation reduced the male-female performance and learning difference substantially and elevated women's modal grades from the C to B range. Benefits were strongest for women who tended to endorse the stereotype that men do better than women in physics. A brief psychological intervention may be a promising way to address the gender gap in science performance and learning.

The substantial underrepresentation of women in science, technology, engineering, and mathematics (STEM) disciplines has long concerned policy-makers and the educational community (*1*, *2*). In 2006, women earned only 28% of Ph.D.s in physical sciences, 25% in mathematics and computer science, and 20% in engineering in the United States (*3*). Although women made up 47% of the North American workforce in 2009, the percentage of women in lucrative technical professions, such as "computer and mathematical occupations" and "architecture and engineering occupations," reached only 25% and 14%, respectively (*4*). Similar underrepresentation of women in STEM-related professions is also evident in other parts of the world (*5*).

The gender gap in STEM disciplines goes beyond the limited representation of women. In college physics—the field studied in the present investigation—women earn lower exam grades and lower scores on standardized tests of conceptual mastery (*6*, *7*). Students' prior background and preparation in mathematics and physics, iden-

[1]Department of Psychology and Neuroscience, University of Colorado at Boulder, Boulder, CO, USA. [2]Department of Physics, University of Colorado at Boulder, Boulder, CO, USA. [3]School of Education, Department of Psychology, and Graduate School of Business, Stanford University, Palo Alto, CA, USA.

*To whom correspondence should be addressed. E-mail: akira.miyake@colorado.edu